Modeling Spatio-Temporal Pattern of Drought Using Three-Dimensional Markov Random Field

Virat Shukla, N. R. Patel, V.A. Tolpekin and V. K. Dadhwal

Abstract

Droughts are major natural disasters for many parts of world. Dry areas, where precipitation pattern is markedly seasonal, or is otherwise highly variable, are the most susceptible. Unlike most natural disasters, drought onset is difficult to identify. Meteorological and agricultural drought occurrences along time and space take place randomly and therefore their scientific quantifications are possible by the probabilistic methods. In the present work an effort has been made to derive drought pattern using spatio-temporal information by the use of temporal images from NOAA-AVHRR based Normalized Difference Vegetation Index (NDVI) and meteorological based Standardized Precipitation Index (SPI). In this study we propose a spatio-temporal explicit algorithm called as Three-Dimensional Markov random field model for the identification of drought pattern at next moment of time. This algorithm is based on the assumption that Standardized Vegetation Index (SVI) reflects the state of vegetation at the given moment and SPI influences the state of vegetation in the future, this effect was modeled by incorporation of spatio-temporal contextual information in terms of energy function. The algorithm is initialized by the calculation of class temporal prior probability from the temporal images. Finally, an iterative algorithm, Simulated annealing, was used to compute global posterior energy for all possible updates of the class labels and new class label was chosen that correspond to lowest energy value. A difficult issue related to MRF is the determination of the (Markov Random Field) MRF model parameters that weight the energy terms related to the available information sources. The concept of minimum perturbation was used to estimate the parameters value.

Key words: Markove Random field, Drought, Standardized Vegetation Index, Standardized Precipitation Index

Introduction

Drought is complex event which may impair social, economic, agricultural and other activities of society. It is temporary, recurring natural disaster, which originates from the lack of precipitation and brings significant economic losses. It is a slow poison, no one knows when it creeps in, it can last any number of days and its severity cannot be predicted. The non-structural characteristic of drought impacts has certainly hindered the development of accurate, reliable, and timely estimates of severity and ultimately, the formulation of drought preparedness plans by most governments. The impacts of drought, like those of other hazards, can be reduced through mitigation and preparedness. Defining drought is difficult; it depends on differences in regions, needs, and disciplinary perspectives. Drought always starts with the lack of precipitation, but may (or may not, depending on how long and severe it is) affect soil moisture, streams, groundwater, ecosystems and human beings. This leads to the identification of different types of drought (meteorological, agricultural, hydrological, socio-economic, ecological), which reflect the perspectives of different sectors on water shortages. India is predominantly an agrarian country as more than 70% of its population is dependent on agriculture. Rainfall is the main source of water for agriculture. Drought is measured in terms of meteorological drought. It is well known that the supply of water through rainfall cannot be as regular as it can be through irrigation. The drought of 1987 was one of the worst in the century. Gujarat is one such state where drought occurs with unfailing regularity. Gujarat is chronically dry and prone to drought. Drought in the state is the result of a combination of natural factors, principally the scarcity of rain, and man-made factors such as deforestation and overgrazing, the absence of traditional rainwater harvesting systems etc. In 1999, as many as 98 out of a total of 225 blocks in the state received less than 50% of the season's expected rainfall. In 1999, Gujarat faced the worst drought of the past 100 years.

The impact of drought on society and agriculture is a real issue but it is not easily quantified. Reliable indices to detect the spatial and temporal dimensions of drought occurrences and its intensity are necessary to assess the impact and also for decision-making and crop research priorities for alleviation (Seiler et al., 1998). The development and advancements in space technology, to address issues like drought detection, monitoring and assessment have been dealt with very successfully and helped in formulation of plans to deal with this slow onset disaster. With the help of environmental satellite, drought can be detected 4-6 weeks earlier than before and delineated more accurately, and its impact on agriculture can be diagnosed far in advance of harvest, which is the most vital for global food security and trade (Kogan, 1990). Recent literature shows that among the meteorological drought indices, the Standardized Precipitation Index (SPI) is relatively new index that has gained wider acceptance over others in India (Chaudhar1 and Dadhwal, 2004) and worldwide (Gutman, 1998; Hayes et al., 1999; Vicente-Serrano et al., 2004; Wu et al., 2005) This popularity of SPI is mainly due to its robustness, temporal flexibility and effectiveness to represent both wet and dry spells at different time scales. This index captures the accumulated deficit (SPI < 0) or surplus (SPI > 0) of precipitation over a specified period of time and provides a normalized measure (i.e. spatially invariant Z score) of relative precipitation anomalies at multiple time scales. Seasonal timing of measurements is an important factor in the understanding of vegetation vigour and precipitation relationships, and should be taken into account. Recently, (Peters et al., 2002) described the Standardized Vegetation Index (SVI), which is calculated using a Z score and converted to a probability value to evaluate vegetation and drought status with in growing season.

Forecasting of when a drought is likely to begin or to come to an end is extremely difficult. A better characterization of droughts through drought indices is essential to support appropriate monitoring and prediction tools, which allow for drought warning. The Markov chain approach was used by (Lohani and Loganathan, 1997) and (Lohani et al., 1998) to develop an early warning tool. These authors adopted a non-homogeneous Markov chain formulation to derive drought characteristics and assess dry spells from long-term records of the PDSI in two climatic areas of Virginia (USA). (Sen, 1998) proposed two probabilistic models for drought characterization, regional persistence and multiseasonal respectively. They conclude that drought occurrences are dependent on the regional and temporal dry and wet spell probabilities as well as size of the region considered. (Steinemann, 2003) adopted six classes of severity, from wet to dry conditions, relative to the PDSI and the SPI, and used the homogeneous Markov chain formulation to characterize the steady-state probabilities, and the probabilities for drought class transition and for duration in a class. The results obtained allowed the author to propose triggers for activating drought preparedness plans at the basin scale. Other Markov chains applications were recently published but concern dry spells, not early warning.

Markov Random Fields (MRF) are commonly used probabilistic models for image analysis (Li, 2001). The basic idea of MRF is to model the contextual correlation. Indeed, focusing on classification-based image analysis, it has been shown in the literature that the integration of the context into a classification scheme can significantly improve the results in terms of accuracy and reliability. The first work on MRF based statistical methodology for image analysis application was employed by Geman and Geman in the year 1984 (Li, 2001). Solberg et al. (1996) proposed MRF based model for classification of multi-source satellite imagery. Their model exploits spatial class dependencies between neighbouring pixels in an image, and temporal class dependencies between different images of the same scene. They also compare the performance of MRF based model with simpler reference fusion model. The MRF models had been widely used in image change detection. In order to increase the accuracy of the final change detection map, (Bruzzone and Prieto, 2000) integrated spatial contextual information in their unsupervised change detection scheme through an MRF model that exploits interpixel class dependences to model the prior probabilities of change and no-change classes, by including the temporal aspect of the data, the model was found to be suitable for detection of class changes between the acquisition dates of different images. (Bruzzone and Prieto, 2002) also developed an MRF-based adaptive semi parametric technique that makes use of the Reduced parzen estimate (RPE) and the E-M algorithm to estimate in an unsupervised way the changes that may occur in a temporal sequence of images. (Kasetkasem and Varshney, 2002) addressed the problem of image change detection based on MRF models. They modelled MRF by using noise lese images obtained from the actual scene and change images in order to search for an optimal image of changes by applying the maximum a posterior probability (MAP) decision criterion and the Simulated Annealing energy minimization procedure. (Kasetkasem et al., 2005) employed MRF for land cover mapping at sub pixel level. They proposed method that was able to generate super-resolution land cover maps from remote sensing data. (Liu et al., 2006) proposed a spatial-temporal classification algorithm for forest disease monitoring that explicitly classify individual images using spectral, spatial and temporal information. They concluded that MRF can be used as efficient probabilistic models for the analysis of spatial and temporal contextual information. Thus it can be conclude that these reviews highlight the numerous efforts made till date with developing relationship between various satellite and meteorological derived indices to point out a specific type of drought caused either by rainfall deficiency, or less vegetation vigour or low agricultural production. In the present study, both meteorological indices (SPI) and satellite based drought indices (SVI) have been used to assess the drought. Drought has spatio-temporal behaviour. So it is important to study the temporal as well as spatial nature of drought. The previous study provides a basis for analytical investigation of spatio-temporal pattern of droughts. The main objective of the research was to build a tool for identification of spatio-temporal pattern of drought using Three-dimensional Markov random field. The study was focused on three major areas: 1) quantification of drought classes using NDVI and rainfall datasets in terms of data descriptor. 2) Incorporation of

NDVI and rainfall datasets in three-dimensional Markov Random field. 3) Method to be used for parameter estimation of three-Dimensional Markov random field model.

The outcome of this research provides the users with guidelines on the parameters setting of the Markov random field model. The result obtained using Three-dimensional Markov random field encourages the end users to apply the technique in remotely sensed image with respect to spatio-temporal aspect of the drought to provide more meaningful and understandable information. This kind of information is essential for a broad group of users within the geo-informatics society who are interested in monitoring, mitigation and management of drought. Therefore, this research adopt Three-dimensional Markov random field to model spatio-temporal pattern of drought.

Theoretical Background

Markov Random Field Model

Meteorological and agricultural drought occurrences along time and space take place randomly and therefore their scientific quantifications are possible by the probabilistic methods. Herein Drought characteristics of any phenomenon are assumed to have spatial and temporal stationarity with underlying independent generating mechanism and can be modelled by suitable technique. In interpretation of drought condition, context is very important. Contextual information is ultimately necessary in the interpretation of visual information. It is one kind of spatial relationship and has drawn our particular interest for remotely sensed imagery interpretation shown in this study. Contextual information, or so-called context for simplicity, may be defined as how the probability of presence of one object (or objects) is affected by its (their) neighbours. It may be derived from spectral, spatial or even temporal attributes. In this study, the spatial and temporal dimension has been focused upon. Spatial context shows the spatial relationship between spatially neighbouring pixels within the predefined neighbourhood system. The temporal dimension is defined between the multiple images of the same area. A scene is understood in the spatial and visual context of the objects in it; the objects are recognized in the context of object features.

Using concept of context, pixel in the image are not treated in isolation, but are considered to have relationship with their neighbours. Thus the relationship between pixel of interest and its neighbours are treated as being statistically dependent. A nearest neighbourhood dependence of pixels on an image lattice is obtained by going beyond the assumption of statistical independence. Information on the nearest neighbourhood is used to calculate conditional probabilities.

Generally, in drought Modeling through remote sensing, a pixel labelled as class of moderate drought is likely to be surrounded by the same class of pixels unless it is located on the boundary. Incorporating contextual information into Drought Modeling can be done in different ways. One simple method of adopting context is to use majority voting within a prescribed window. In such a method, the central pixel will be changed to the class that occurs most frequently in the window. There are more elegant ways of Modeling such contextual behaviour.

A class of contextual model known as Markov random field (MRF) can be useful for Modeling context in a more precise way .It is a probabilistic model defined by the local conditional probabilities. Markov random field (MRF) theory provides a convenient and consistent way for Modeling spatial-temporal contextual information in terms of conditional prior probabilities. MRF is used to construct a priori probability in Bayesian sense so as to accomplish the Maximum a Posteriori (MAP) estimate during the Modeling process. Maximum a posterior (MAP) probability is one of the most popular criteria for optimality and widely applied for MRF Modeling (Li, 2001).

Study Area and Data sets

The Gujarat State is situated on the western coast of India between 20º06' to24°42' north latitudes and 68°10'N to 74°28' east longitudes which is shown in Fig1.

Figure 1: Gujarat map showing Weather monitoring Stations.

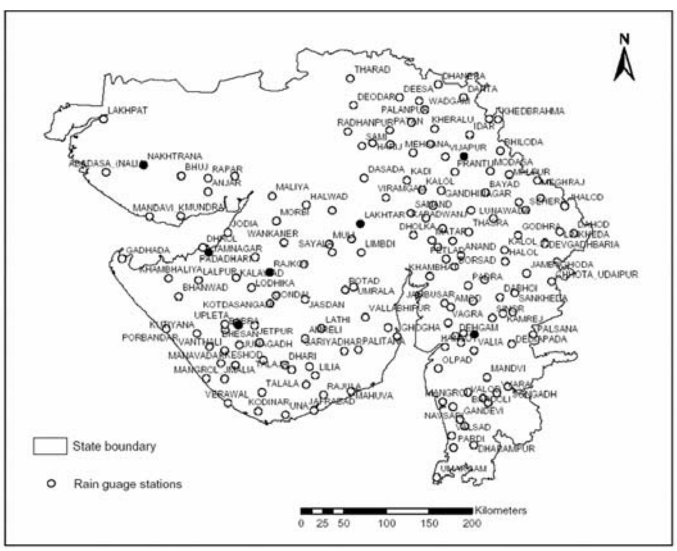

It comprises of 25 districts with a total geographical area of 1.96 lakh square kilometers. It has a 1600 km long coast-line. The Gujarat state has been divided into three major physiographic regions, namely the Central Highlands, the Western Hills and the West Coast. The extreme part of the state is occupied by the Central Highlands, a wide belt of hilly region bordered by the Arravali Range on the west. The Western Hills forms the part of the peninsular plateau while the Western Coast covers major portion of the state, comprising of Gujarat Plain, Kathiawar Peninsula and Kutch Peninsula. Deltaic plains by the alluvium laid by the Tapi, Narmada, Mahi, Sabarmati, Banas and Luni river systems have lead to the formation of Gujarat Plains progressively. Kathiawar Peninsula is a dissected basaltic plateau with flat-topped hills of Mesozoic sandstones in the northeast while the central part forms a high plateau bordered by scarps and dotted hills.

The climate of Gujarat is also varied and can be divided into three seasons: (1) hot and dry season from May to June; (2) warm and rainy season from June to September; and (3) cool and dry post-rainy season from October to April (Agro climatology of Gujarat). The north-western part of the state is dry, with less than 500 mm of rain every year. In the more temperate central part of the state, the annual rainfall is more than 700 mm. In the southern part, rainfall averages 2000 mm a year. Gujarat is endowed with a wide range of soil type. The state is divided into seven agro climatic zones mainly based on amount of rainfall and soil types. Landuse is one of the driving forces behind water demand and critical factors of agricultural drought vulnerability. Agriculture in Gujarat forms a vital sector of the states economy.

Data

Data has been acquired mainly from two sources, firstly NDVI derived from satellite sources and secondly rainfall obtained from ground rainfall stations. The monthly time series of NDVI data set for the period of 1981-2003 was taken into consideration. The time series of NOAA-AVHRR based fortnightly NDVI composite created by Global Inventory Modeling and Mapping studies (GIMMS) Group at NASA's Goddard Space Flight Center (Tucker et al., 2005).The composite images covering Eurasia (EA) was downloaded and subset corresponds to Gujarat was extracted from continental data sets. Monthy NDVI data set derived by taking maximum of fortnightly NDVI at a spatial resolution of 8km. Monthly rainfall datasets were acquired for the period of 22 years ranging from 1982-2003 for the Gujarat state. Monthly rainfall for 164 rain stations has been used to derive Standardized Precipitation Index (SPI). The data has been collected from Bhaskaracharya Institute of Satellite and Geoinformation (BISAG), Gandhinagar and Agro-Meteorological Department, Anand Agriculture University, Anand. Many experiments were performed to obtain the optimal parmeters value. To estimate the parameter value, training dataset was used and the corresponding result was validated with the reference data.

Methodology

The methodology developed for modelling spatio-temporal pattern of drought is as shown in Fig 2 and discussed in following sections.

Figure 2: Schematic representation of steps involved in modeling spatio-temporal pattern of drought using 3D Markov Random field Model.

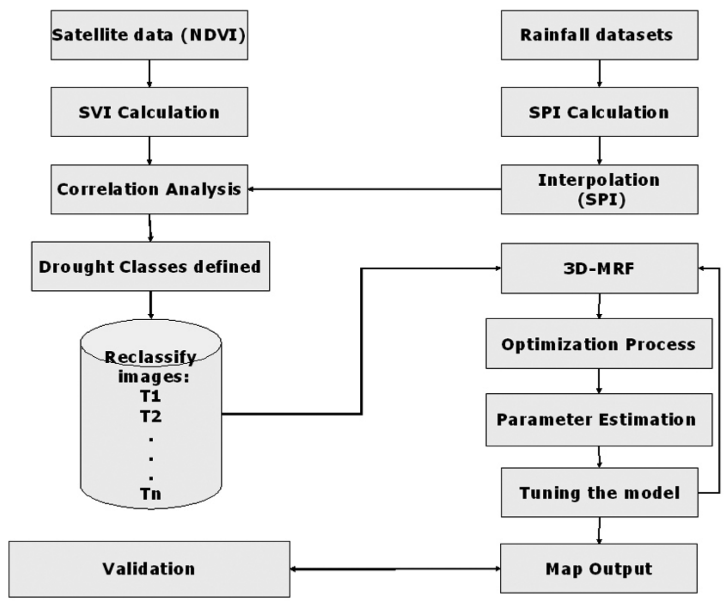

All the twenty two years of NDVI-AVHRR datasets were used for the calculation of SVI. As mentioned earlier SPI was developed to quantify precipitation deficit at different time scales. SPI was interpolated for five months i.e. June, July, August, September and October for the time period from 1982 to 2003. A geostatistical technique of interpolation i.e. Ordinary kriging was performed with grid size of 8 Km and seasonal maps for 22 years were prepared. The spatial continuity of the data was examined on the basis of the variogram analysis. Variogram for different months were made to get the sill, range, partial sill and nugget. Considering the lag effect, correlation analysis was carried between SPI and SVI in order to establish the relationship. Based on the relationship between SPI and SVI, thresholds to categorize drought classes from SVI were defined. Optimization process was carried using simulated annealing algorithm. Finally parameter estimation and Tuning of the Three-dimensional Markov Random field model was done in order to validate the result.

Computation of Standardized Vegetation Index and Standardized Precipitation Index

All the twenty two years of NDVI-AVHRR datasets were imported to ENVI 4.1 and compositing process was carried out to select the pixels with high NDVI values to get a cloud free image. NOAA-AVHRR- NDVI data sets from 1982 to 2003 was used to calculate the Standardized Vegetation Index. The SVI is based on calculation of a Z-score for each AVHRR pixel location. The Z-score is a deviation from the mean in units of the standard deviation, calculated from the NDVI values for each pixel location for each month for each year, during the n-years as

$$Z_{ijk} = \frac{(NDVI_{ijk} - NDVI_{ij})}{\sigma_{ij}}$$

Where,

Z_{ijk} = Z-Score

$NDVI_{ijk}$ = highest NDVI value for pixel i during month j for year k,

$NDVI_{ij}$ = mean NDVI for pixel i during month j over n years

σ_{ij} = standard deviation of pixel i during month j over n years.

After the calculation of Z- score for each pixel, the probability of that score was determined as

$$SVI = P(x \prec Z_{ijk})$$

This per pixel probability is expressed as the Standardized Vegetation Index (SVI), is an estimate of the "probability of occurrence" of the present vegetation condition which was calculated using the program that was written in IDL 6.1.

Monthly Rainfall data for 164 rainfall stations were arranged according to format defined by (National Drought Mitigation Center, 2006) to have input to SPI program. SPI was computed for each station on time scale 1, 2, 3, 6, 9 and 12. This index is calculated by fitting gamma distribution to observed values of precipitation at different time steps (e.g. 1 month, 2 months, 3 months… 48 months) and then transform back to normal distribution with mean zero and variance one. The SPI was designed to quantify the precipitation deficit for multiple time scales. SPI at different time scale e.g. 1-month or

3-months SPI of particular month represents deviation in precipitation totals for same month and current plus previous two months, respectively.

Three-dimensional Markov Random field Model Framework

Consider a Set S that denotes the set of sites defined over an image. The sites in S are related to one another via a neighbourhood system. A neighborhood system for S is defined as:

$$N = \{N_i \mid \forall i \in S\}$$

Where *Ni* is the set of sites neighboring *i*. The neighborhood system has the following properties:

(1) A pixel can not be a neighbour to itself.

(2) The neighbouring relationship is mutual.

In the first order neighbourhood system, also called the 4-neighborhood system, every site has 4-neighbors which share a side with the given site. In Second order neighbourhood system, every site has 8-neighbors which share a side with the given site. Although it is possible to use various spatial neighbourhood systems, Second order neighbourhood is considered to be enough in some of the previous MRF studies (Hailu Kassaye, 2006; Kasetkasem et al., 2005; Kasetkasem and Varshney, 2002). Hence, a second order neighbourhood system or window size 3 was considered in the present research. The Fig 3 shows the spatial-temporal neighbourhood system used in this study. The nomenclature used to represent theoretical and mathematical formulation of 3-D Markov Random Field Model is mentioned in Table 1.

Figure 3: MRF neighbourhood systems (Note: spatial neighbourhood (Left); spatio-temporal neighbourhood. Axes X, Y are the spatial coordinates of sites. Axis T is the temporal index of the sites (Right).)

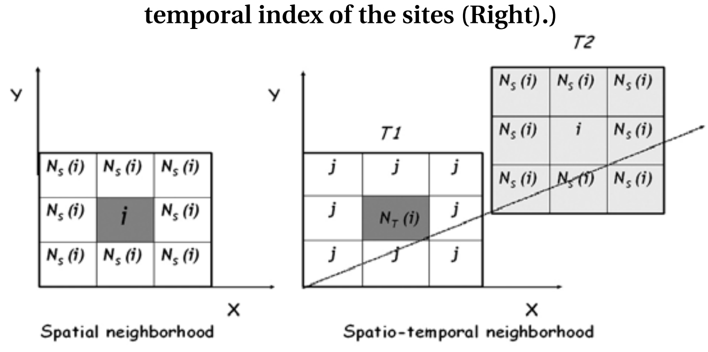

Table 1 Nomenclature used in defining 3-D Markov random field model

Symbol	Explanation
c (i, t)	Class value of site i at time t, class is defined as drought class based on SVI
d (i, t)	Class value of site i at time t, class is defined as drought class based on SPI
U sp	Spatial prior energy function
U td	Temporal Dependence energy Function
ct	Set of class labels for the scene at time t
c (Ns (i, t))	Class vector of Spatial neighbourhood of site i at time t
Z	Normalizing constant also called partition function
Model Parameters	
β_{sp}	Parameter to control the spatial energy
β_{td}	Parameter to control the temporal dependence energy

Formulation of the Objective Function

Spatial Energy Function

The spatial energy was defined as favoring small changes in the drought class and penalizing the large ones. The spatial energy function encourages neighbouring pixels to β_{SP} be classified with the same labels and thus impose a spatial smoothness effect. Both the spatial and temporal energy functions require the definition of a neighbourhood system. In our case, a second-order neighbourhood system is adopted. Specifically, the spatial energy function involved in MRF is specified as:

$$U_{sp}\left(c(i,t), c\left(N_s(i,t)\right)\right) = \beta_{sp} \sum_{j \in N_s(i)} \left(c(i,t) - c(j,t)\right)^\wedge 2$$

Where,

U_{sp} is spatial energy function

c(i,t) denote the drought class of site i at time t based on SVI.

c(N_S(i,t)) denote the neighbouring drought class of site i at time t based on SVI.

is a non-negative parameter controlling the spatial dependence

Temporal dependence energy function

Temporal neighbors contribute to the energy function in a probabilistic sense which is specified by transitional probability concept. In our spatial-temporal approach, the temporal relation is modeled by a transition probability matrix which defines the probability of one pixel belonging to one drought class at a time T1 given that it belongs to another class at time T2. Specifically the temporal dependence energy function in MRF model is formulated as

$$U_{td}\left(d(i,t_1), c(i,t_2)\right) = -\beta_{td} \cdot \ln\left(P(c(i,t_2) \mid d(i,t_1)\right)$$

U_{td} is temporal dependence energy function.
$d_{i,t1}$ denotes the drought class of site i at time t1 based on SPI.
$C_{i,t2}$ denotes the drought class of site i at time t2 based on SVI.
$(P(c(i,t_2)\,|\,d(i,t_1))$ is the transitional probability of $d(i,t_{t1}) \Rightarrow c(i,t_2)$
Bayes statistics is a theory of fundamental importance in estimation and decision making.

When the context is introduced as prior information and modeled by means of MRF, Bayesian framework can be adopted to construct the global energy and labeling is carried out by minimizing this global posterior energy, since energy and probability are inversely proportional, one can say that the lower the energy the higher is the probability of labeling. Information on the nearest neighborhood is used to calculate the conditional probabilities. In this study we applied the assumption of MRF being isotropic and homogeneous for the neighboring pixels in the same neighborhood order. The global posterior energy is defined as:

$$U_{Global=}U_{sp} + U_{td}$$

Where U_{Global} is global posterior energy.
The optimal class label $\hat{w}_j$ can be found by minimizing the global posterior energy, to get the optimal solution maximum a posterior (MAP) was adopted as:

$$\hat{w}_j = \underset{w_j \in c(i,t)}{Min}\left(U^i_{Global}\left(w_j\right)\right)$$

After the construction of the global posterior energy, the next step was to perform pixel labeling by minimizing the global posterior energy. One would like to obtain a pixel labeling that is reasonable to the data and the prior model. A popular criterion is to find the labeling that maximizes the posterior distribution (MAP). Three algorithms, namely Iterated conditional modes (ICM), Maximum a Posterior Marginals (MPM) and Simulated Annealing (SA) can be used to obtain global minimum energy. These algorithms are iterative in nature.

Simulated annealing algorithm was adopted to find the MAP solution. Simulated annealing is a type of stochastic algorithm for combinatorial optimization. The concept of simulated annealing is equivalent to the introduction of the noise in to the system to shake the search process away from the local minimum. The idea is similar to a process in metallurgy in which a small region of a metal structure is heated until it is pliable enough to be reconstructed in to the desired shape. The metal is then cooled very slowly to make sure that it is given enough time to respond. Changes in temperature must be very small until the metal is hardened. The whole process is controlled by initial temperature and updating schedule. Initially the process is started at high temperature; this means that a high temperature can increase the probability of a pixel being replaced by new class label even though the new class label has high energy. The temperature is decreased according to predefined cooling schedule. In this study we adopted following equations for the cooling schedule.

$$T = \frac{T_0}{\log(1 + beta(K + 1))}$$

Where T_0 is initial temperature

beta is a constant which represents how much the temperature would decrease for every iteration. It is called as descent constant or other wise called as "Rate of fall".

K denotes the number of iteration.

The pixel updating was performed according to the energy difference between old class label and new class label. If the energy of the old class label was higher than the new class label, than pixel was replaced by the new class label. The iteration was repeated for each temperature update value.

The MRF models make use of parameters that weigh the influence of information sources on the decision process. This can be viewed as a way of expressing the degree of confidence (reliability) in each information source. In practice, the MRF parameters permit one to "tune up" the MRF model in order to get optimal solution. The determination of the MRF parameters is not a trivial problem. The larger the number of information sources, the larger the number of MRF parameters and the more difficult the parameter estimation. In this study, minimum perturbation method was used to estimate the MRF parameters. Let us consider image consists of M sites i.e. S_i (i= 1 … M).The first step of the method consists in computing the total energy associated with each pixel i.e. class label w_j (j = 1, 2… 5) associated with that pixel, under the assumption that all the information sources have the same reliability weights. In other words, the following energy is computed for each pixel associated class label.

$$U^i_{Global}(w_j) = U^i_{sp}(w_j) + U^i_{td}(w_j)$$

The optimal class $\hat{w}_i$ for the site S_i is one that satisfies

$$U^i_{Global}\left(\hat{w}_i\right) = \underset{w_j \in c(i,t)}{Min}\left(U^i_{Global}(w_j)\right)$$

The "minimum energy perturbation" is defined as the smallest additional amount of energy required to classify the Pixel class label correctly (Melgani and Serpico, 2003).

$$\Delta U^{i} = \left[U^{i}_{Global}\left(\hat{w}_{j}\right) - U^{i}_{Global}\left(w_{j}\right) \right] \times (1+\delta)$$

Where w_i stands for the true class of the pixel i and d is an arbitrary small positive constant. In case the optimal class $\hat{w}_j$ should correspond to the true class w_j, the minimum perturbation energy would become null. Then after the computation of the minimal energy perturbation for each pixel class label, the second step of method consists in estimating the values of parameters that satisfy the following systems of equations:

$$\begin{bmatrix} U^{1}_{sp}\left(w^{1}_{t}\right) & U^{1}_{td}\left(w^{1}_{t}\right) \\ U^{2}_{sp}\left(w^{2}_{t}\right) & U^{2}_{td}\left(w^{2}_{t}\right) \\ . & . \\ . & . \\ U^{m}_{sp}\left(w^{m}_{t}\right) & U^{m}_{td}\left(w^{m}_{t}\right) \end{bmatrix} \cdot \begin{bmatrix} \beta_{sp} \\ \beta_{td} \end{bmatrix} = \begin{bmatrix} T^{1} \\ T^{2} \\ . \\ . \\ T^{m} \end{bmatrix}$$

Where T^i (i = 1… m) given by

$$T^{i} = U^{i}_{t}\left(w^{i}_{t}\right) + \Delta U^{i}$$

To find an approximate solution for such a system characterized by a number of equations larger than the number of unknowns is to adopt the minimization of the sum-of-squared error as a criterion and to apply the technique based on the pseudo-inverse matrix for its optimization. By rewriting the system of equations in terms of matrices:

$$\bar{U} \cdot \bar{\beta} = \bar{T}$$

To estimate the optimal MRF parameter vector β^{*} is given by the following expression based on the pseudo-inverse of the matrix U:

$$\beta^{*} = \left(U^{tr} U\right)^{-1} U^{tr} \bar{T}$$

Where tr is transpose of the matrix.

The method is applied in the context of the initialization step of the simulated annealing algorithm.

Results and Discussion

The relationship between vegetation and moisture availability was clarified by analyzing the co variation of SVI and SPI time series with the scatter plots and correlation analysis. SVI time series data for each of the 164 rain stations was extracted from the 22 years SVI time series images. Correlation coefficient between SPI and SVI was calculated. Generally there is a time lag between precipitation events and response of vegetation to such events. The time interval between a precipitation event and the time when precipitated water might reach a plant root and affect plant growth can vary from 1 to 12 weeks depending on vegetation type (Ji and Peters, 2003). In order to account for this interval and assess the real maximum correlation between SVI and SPI the SVI/rainfall correlation coefficients were calculated for time lags of 0,1 and 2 months. Out of three lag-time, the correlation coefficient for time lag of 1 month was found to be higher than others one. (Rundquist et al., 2000) found the lag time of vegetation response to precipitation was approximately 1 month. Mathematically the relation can be written as following:

$$SVI_t \approx f\left(SPI_{t-1}\right)$$

Where *t* denotes month.

Representative points for agro-climatic zones of Gujarat were selected for analysis. Correlation analysis was carried out for the month of June to October between SPI and SVI from the period 1982-2003 to analyze the temporal pattern of SPI and SVI and to see variation in vegetation according to rainfall. It can be noted from the Table 2 that significant correlation exists between SPI and SVI in different months.

Table 2: Correlation analysis between SPI and SVI for time lag of 1-month

STATION NAME	SPI(JUNE) -SVI (JULY)	SPI(JULY) - SVI (AUGUST)	SPI(AUGUST) - SVI (SEPTEMBER)	SPI (SEPTEMBER) - SVI (OCTOBER)
NAKHTRANA	0.06	0.56	0.317	0.57
HIMATNAGAR	0.49	0.144	0.46	0.72
JHAGADIA	0.47	-0.08	0.14	0.12
LAKHTAR	0.40	0.05	0.29	0.14
DHORAJI	0.24	0.03	0.39	0.37
JAMNAGAR	0.45	0.19	0.48	0.26
RAJKOT	0.19	0.28	0.52	0.29

When comparing the correlation coefficients with the vegetation phonological cycle, it is clear that vegetation response to moisture availability varies significantly between months. Correlation between SPI and SVI on lag effect was found to be positive in north and northern-western part of Gujarat for all months. Reason behind positive correlation could be because of rain fed crops. The lowest correlation values appear in south Gujarat, which is high rainfall area (1000 mm - 2500 mm) where as high correlation (> 0.4) is vigilant in arid and semi-arid areas of north Gujarat and central part of Kathiawar peninsula. These are the areas where annual rainfall is between 400- 700 mm. maximum correlation values are obtained in this region because precipitation event serves as primary source of water for plant growth.

Generalized Classification of the Drought Classes

The generalized classification of the drought classes was done based on the observed relationship between SPI and SVI. All the SPI and SVI images were reclassified accordingly. For the Standardized Vegetation index (SVI) images, five drought classes have been defined in terms of data descriptor. In order to implement the MRF model and for simplicity the drought classes were reclassified. So images consist of only numbers i.e. 1, 2, 3, 4 and 5. Each number corresponds to different drought class. Generalized classification of drought class was done which is shown in Table 3.

Table 3 Generalized classification of drought classes

SPI VALUES	DROUGHT CLASS
-2 to less	Severe drought
-1.5 to -1.99	Moderate drought
-1.0 to -1.49	Slight drought
-0.99 to 0.99	Normal
1.0 to 2.0+	Favourable
SVI threshold	Drought Class
0 - 0.10	Severe drought
0.10 - 0.25	Moderate drought
0.25 - 0.5	Slight drought
0.5 - 0.75	Normal
0.75 - 1	Favourable
SPI and SVI values\Reclassification	
Severe drought	1
Moderate drought	2
Slight drought	3
Normal	4
Favourable	5

Several attempts were made to understand and illustrate the capability of three-dimensional Markov random field model for identification of drought pattern at next time moment using spatio-temporal information. To identify the pattern of drought at next time, initially the class temporal prior probability was calculated by considering the temporal images for each pixel values. That class label was chosen which maximize the class temporal probability. It was done in order to get an image that can be used as an initial image for the optimization process. The spatial energy function encourages neighboring pixels to be classified with the same class labels and thus imposes a spatial smoothness effect on the final prediction. The temporal dependence energy function was calculated in terms of transitional probability, thus updating the prediction with important source of information, then at each step updating of class label was done in such a way that global posterior energy is minimized. So global posterior energy i.e. spatial energy function and temporal dependence energy which involves the pixel of interest was computed for all possible updates of the class labels and new class label was chosen that correspond to lowest energy value. The replacement of old class label with new one was done and then the model proceeds to next pixel. If the optimal class label was the same as before the update, then it was not considered as a successful update. Otherwise it was considered as a successful update. During optimisation process, different experiments were performed to obtain the optimal parameters value using different training datasets. Several attempts were made to find good set of MRF parameters. Few experimental results are discussed in next subsection

Experiment 1: An experiment was performed to obtain the optimal parameters value. The initial temperature was set to 100. To estimate the parameter value, training dataset was used. An image of SPI, June 1987 was used. For the initialization purpose the image from 1982 to 1986 of SVI July was used to calculate the temporal class probability. During this process the temperature is lowered slowly until it reaches to a freezing state. The optimization process converges to minimum energy after 32 iterations. The optimal parameters value obtained are:

β_{sp} = 0.0162306 and β_{td} = 0.377119

Using the above parameters value, the estimation of SVI 1987, July, August, September and October was done. SVI July 1987 prediction matches with reference data which is shown in Fig 4.

Experiment 2: In another experiment the initial temperature was set to 100. To estimate the parameter value, training dataset was used. An image of SPI, August 2002 was used. For the initialization purpose the image from 1982 to 2001 of SVI September was used to

Figure 4: Predicted image of SVI July 1987 (Left) and Reference data- SVI July 1987 (Right) for experiment 1.

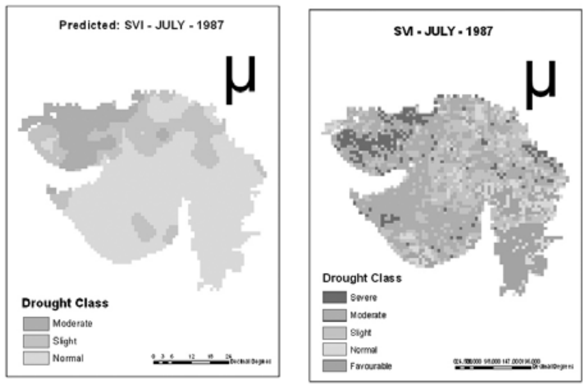

calculate the temporal class probability. During this process the temperature is lowered slowly until it reaches to a freezing state. The optimization process converges to minimum energy after 66 iterations. The optimal parameters value obtained are:
β_{sp} = 0.00048, β_{td} = 0.128913

Using the above parameters value, the estimation of SVI 1987, July, August, September and October was done. The predicted SVI July 1987 and the corresponding reference data is shown in Fig 5.

Figure 5: Predicted image of SVI July 1987 (Left) and Reference data- SVI July 1987 (Right) for experiment 2.

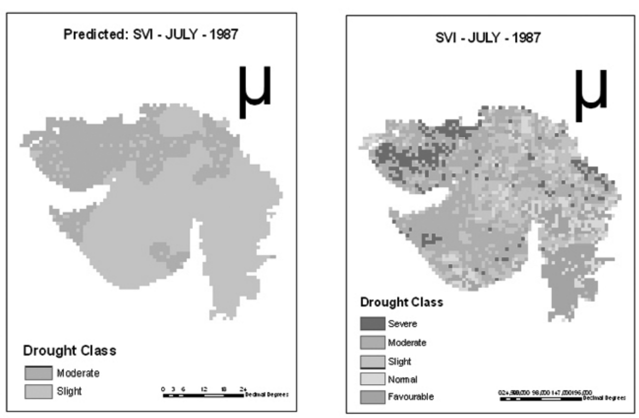

From the results it is concluded that there is no unique optimal parameter value that can optimize the prediction quality of all transitions of all possible data. The reason for not getting the required result depends on how well the relationship is defined between SPI and SVI. The relationship between the SPI and SVI has affected the model output because the model was implemented according to the assumption that the SVI reflects the state of vegetation at the given moment and SPI influences the state of vegetation in the future, this effect was modeled in terms of energy function in the MRF. If the output of a model is not what was expected, there are two possible reasons:

- The formulation of the objective function was not appropriate one for Modeling the complex phenomenon like drought.
- The output was a low quality local minimum

The most important aspects of the energy function are its form, involved parameters and the corresponding assumptions made during the Modeling. The form and parameters together define the energy function which in turn defines the minimal solution. The form and parameters depends on the assumption about the expected solution and the observed data. Since the parameters are part of the definition of the energy function, the solution is not completely defined if the parameters are not specified even if the functional form is known. The above mentioned reason may deviate the solution from the expected.

Selection of factors that affect the drought Modeling is also a crucial component. The factors such as soil moisture, temperature, evaporation, relative humidity, evapo-transpiration, wind speed affect the drought Modeling. One of possible reason for not getting the expected output was the above mentioned constraints or factors which affect the drought prediction was not embedded in to the energy function. The energy functions defined in this study was done using only first order approach. This may be one of the possible reasons that affect the output.

Conclusions

The main objective of the study was to build a tool for identification of drought pattern using three-dimensional Markov random field. In order to address the objectives three research questions were posed during this study. Several experiments were carried in order to provide answers for the raised questions. The first research question examine that how to quantify the drought classes using NDVI and rainfall in terms of data descriptor. It was concluded from the study that the temporal variations of SVI are closely linked with precipitation and there exists a significant correlation for time lag of

1 month between SVI and 1-month SPI. It was found that rainfall has positive relation with SVI and also correlation of rainfall/SVI was found to be strong in water limiting areas, which states that these areas are more prone to drought. Based on the relationship between the SVI and SPI, generalized classification of drought class was done and five drought classes were defined. Finally the quantification of drought class in terms of data descriptor was presented. It was found that using SPI one can compare rainfall of two areas with different rainfall characteristics. Thus SPI can be used for the indication of the drought characteristics at the spatial level. NDVI time series was subjected to scale to Standardized vegetation index in order to monitor the drought. By identifying the relationship between SPI and SVI, It was concluded that at some location were SPI was unable to show the drought area, SVI get advantage over SPI. Thus integration and analysis of drought identified areas from SPI and SVI, help in correctly identifying the region affected by drought. The second research question was how to incorporate the NDVI and rainfall in MRF model. The model incorporates the relationship between the SPI and SVI i.e. SVI reflects the state of vegetation at the given moment and SPI influences the state of vegetation in the future, this effect was modeled in terms of energy function in the MRF. The third research question tells about the proper parameter setting in the MRF model and the method adopted for the parameter estimation. Proper parameter setting can lead to a successful result. So it was necessary to search the optimal parameters values. According to the experimental results, it is concluded that there is no unique optimal parameter value which can optimize the prediction quality of all transitions of all possible data. The reason for not getting the expected output depends on the assumptions that were made during the Modeling. The model was implemented according to the assumption that lag time of vegetation response to precipitation was approximately 1 month. From the previous studies, it was found that vegetation response to precipitation was 4-8 weeks depending on the vegetation cover types. Sine the lag time is not known exactly, the output of the model was affected. The validation of model was done with mentioned reference data. The prediction of SVI July 1987 using parameter values 0.0162306, 0.377119 were found optimal for that drought year. The choice of the energy functions has also affected the model output. For the parameter estimation, the simple and fast method "the minimum perturbation energy" was used to get the values. A tool to model spatio-temporal pattern of drought using Three-dimensional Markov random field was developed. The model in the present state worked well with assumption taken in present study. Since drought Modeling is affected by many parameters, the model can be improved by incorporating more parameters (soil moisture, temperature, evaporation, relative humidity, evapo-transpiration, wind speed)

in form of well defined energy function. In general one can conclude that, the ability to extract drought in automated fashion will contribute to further spatio-temporal analysis of drought Modeling. This work using a spatio-temporal explicit algorithm in drought monitoring context has broader applicability across different applications using temporal remote sensing imagery. The overall methodology presented in this paper provides a general framework on the use of spatio-temporal information from NDVI time series data. As such the new method is not limited to the specific data used in this work. However, the spatio-temporal information might vary its value in different applications with different spatial resolution and temporal frequency of images

Acknowledgement

We wish to acknowledge guidance and support received from Dr. Ramachandran and his team, ADRIN, Hyderabad, India for execution of modelling activity.

References

Bavadam, L., 2001. Dealing with drought. *Frontline*, p. 09-22.

Bruzzone, L., and Prieto, D., 2000. Automatic analysis of the difference image for unsupervised change detection. *IEEE Transactions on Geoscience and Remote Sensing*, v. 38, p. 1171-1182.

Bruzzone, L., and Prieto, D., 2002, An adaptive semiparametric and context-based approach to unsupervised change detection in multitemporal remote-sensing images *IEEE Transactions on Image Processing*, v. 11, p. 452-466.

Chaudhari, K. N. and Dadhwal, V. K., 2004, Assessment of impact of drought- 2002 on the production of major kharif and rabi crops using standardized precipitation index. *Journal of Agrometeorology*, v. 6, p. 10-15.

Guttman, N. B., 1998. Comparing the Palmer Drought Index and the Standardized Precipitation Index. *Journal of American Water Resource Association*, v. 34, p. 113-121.

Hailu Kassaye, R., 2006. Suitability of Markov random field based method for super resolution land cover mapping. ITC, *Enschede*, 77 p.

Hayes, M., Svoboda, M., Wilhite, D. and Vanyarkho, O., 1999. Monitoring the 1996 drought using the standardized precipitation index. *Bulletin of the American Meterological Society*, v.80, p. 429-438.

Ji, L. and Peters, A. J., 2003. Assessing vegetation response to drought in the northern Great Plains using vegetation and drought indices. *Remote Sensing of Environment*, v. 87(1), p. 85-98.

Kasetkasem, T., Arora, M. and Varshney, P., 2005. Super-resolution land cover mapping using a Markov random field based approach. *Remote Sensing of Environment*, v. 96(3-4), p. 302-314.

Kasetkasem, T. and Varshney, P., 2002. An image change detection algorithm based on Markov random field models. *IEEE Transactions on Geoscience and Remote Sensing*, v. 40(8), p. 1815-1823.

Kogan, F. N., 1990, Remote-Sensing of Weather Impacts on Vegetation in Nonhomogeneous Areas. *International Journal of Remote Sensing*, v. 11, p. 1405-1419.

Li SZ (2001) Markov Random Field Modeling in Image Analysis. *Springer-Verlag Telos*, 323 p.

Liu, D.S., Kelly, M. and Gong, P., 2006, A spatial-temporal approach to monitoring forest disease spread using multi-temporal high spatial resolution imagery. *Remote Sensing of Environment*, v. 101, p. 167-180.

Lohani, V. and Loganathan, G., 1997. An early warning system for drought management using the Palmer drought index. *Journal of the American Water Resources Association*, v. 33, p. 1375-1386.

Lohani, V., Loganathan, G. and Mostaghimi, S., 1998. Long-term analysis and short-term forecasting of dry spells by Palmer Drought Severity Index. *Nordic Hydrology*, v. 21, p. 21-40

Melgani, F. and Serpico, S. B., 2003. A Markov random field approach to spatio-temporal contextual image classification. *IEEE Transactions on Geoscience and Remote Sensing*, v. 41, p. 2478-2487.

National Drought Mitigation Center, 2006. What is drought, SPI. National Drought Mitigation Center, USA.

Peters, A. J., Walter-Shea, E. A., Ji, L., Vina, A. M., and Svoboda, M., 2002. Drought monitoring with NDVI-based standardized vegetation index. *Photogrammetric Engineering and Remote Sensing*, v. 68, p. 71-75.

Rundquist, B. C., Harrington, J. A. and Goodin, J. D. G.., 2000. Mesoscale Satellite Bioclimatology. *The Professional Geographer*, v. 52, p. 21-28.

Seiler, R, Kogan, F. and Sullivan, J., 1998. AVHRR-based vegetation and temperature condition indices for drought detection in Argentina Remote Sensing: Inversion Problems and Natural Hazards. *Advances in Space Research*, v. 21(3), p. 481-484.

Sen, Z., 1998. Probabilistic formulation of spatio-temporal drought pattern. *Theoretical and Applied Climatology*, v. 61, p. 197-206.

Solberg, AHS., Taxt, T. and Jain, AK, 1996. A Markov random field model for classification of multisource satellite imagery. *IEEE Transactions on Geoscience and Remote Sensing*, v. 34(1), p. 100-113.

Steinemann, A., 2003. Drought indicators and triggers: A stochastic approach to evaluation. *Journal of the American Water Resources Association*, v. 39(5), p. 1217-1233.

Tucker, C. J., Pinzon, J. E., Brown, M. E., Slayback, D., Pak, E. W., Mahoney, R., 2005. An extended AVHRR 8-km NDVI dataset compatible with MODIS and SPOT vegetation NDVI data. *International Journal of Remote Sensing*, v. 26, p. 4485-4498.

Vicente-Serrano, SM., Gonz´alez-Hidalgo, JC., de Luis, M. and Ravent´os, J., 2004. Drought patterns in the Mediterranean area: the Valencia region (eastern Spain). *Climate Research*, v. 26, p. 5-15.

Wu, H., Hayes, M. J., Wilhite, D. A. and Svoboda, M. D., 2005. The effect of the length of record on the standardized precipitation index calculation. *International Journal of Climatology*, v. 25, p. 505-520.